Structural Engineering and Mechanics, *Vol. 52, No. 5 (2014) 857-873*
DOI: http://dx.doi.org/10.12989/sem.2014.52.5.857

Structural behaviors of sustainable hybrid columns under compression and flexure

Wu Xiang-Guo[*1,2], Hu Qiong[1,2a], Zou Ruofei[3b], Zhao Xinyu[4c] and Yu Qun[4d]

[1]*Key Lab of Structures Dynamic Behavior and Control of the Ministry of Education, Harbin Institute of Technology, Harbin, 150090, China*
[2]*School of Civil Engineering, Harbin Institute of Technology, Harbin 150090, China*
[3]*Department of Civil and Environmental Engineering, University of Illinois, IL 61801-2352, USA*
[4]*School of Architecture Engineering, Harbin Engineering University, Harbin 150001, China*

(Received November 28, 2013, Revised April 14, 2014, Accepted April 25, 2014)

Abstract. Structural behaviors of a sustainable hybrid column with the ultra high performance cementitious composites (UHPCC) permanent form under compression and flexure were studied. Critical state and failure stage characters are analyzed for large and small eccentricity cases. A simplified theoretical model is proposed for engineering designs and unified formulas for loading capacity of the hybrid column under compression and flexure loads are derived, including axial force and moment. Non-linear numerical analysis is carried out to verify the theoretical predictions. The theoretical predictions agree well with the numerical results which are verified by the short hybrid column tests recursively. Compared with the traditional reinforced concrete (RC) column, the loading capacity of the sustainable hybrid column is improved significantly due to UHPCC confinements.

Keywords: sustainable design; hybrid column; loading capacity; ultra high performance cementitious composites

1. Introduction

Structural behavior deterioration is serious after decades of service and this often occurs much before the end of the original design life. The most important reason is the relatively low cracking strength and permeability of normal concrete. Worldwide, researchers are making efforts to realize sustainable engineering structure designs. Maalej and Li (1995) proposed substituting the reinforcing steel coat layer with strain hardening Engineered Cementitious Composites (ECC). Based on this design concept, a composite flexural beam with an ECC coat layer was tested in their laboratory. To improve existing bridge pier service life, the Railway Transportation Management Center of China (RTMCC) also proposed the design concept of a pier protection

∗Corresponding author, Professor, E-mail: wuxiangguo@hit.edu.cn
[a]Associate Professor, E-mail: huqiong@hit.edu.cn
[b]Ph.D. Student, E-mail: rzou3@illinois.edu
[c]Ph.D. Student, E-mail: zhaoxinyu@hrbeu.edu.cn
[d]Engineer, E-mail: dacong1986@126.com

Copyright © 2014 Techno-Press, Ltd.
http://www.techno-press.org/?journal=sem&subpage=8 ISSN: 1225-4568 (Print), 1598-6217 (Online)

plate, which has been applied to existing railway bridge piers to improve structural durability (Design code 2009). However, these design concepts only concentrated on retrofitting existing structures. The objective of these retrofitting methods is only to improve the durability of the coat layer, without consideration of improvement of structural behaviors such as cracking load and ultimate load.

A sustainable hybrid column using the ultra high performance cementitious composites (UHPCC) permanent form is proposed to realize high durability and high strength structure simultaneously. UHPCC is obtained by mixing short and thin steel fibers, a high strength cementitious matrix, and mineral admixtures with a special mixing technique and curing system. As a new generation of engineering structural material, UHPCC exhibits high strength (Compression strength 100-200MPa, rupture strength 15-30MPa), high ductility and high durability (Wu and Xu 2009). Recently, a number of researchers have carried out extensive research, such as on the constitutive property behavior of UHPCC (Williams *et al.* 2010), strength model (Ramadoss and Nagamani 2008, Ramadoss and Nagamani 2013), UHPCC behavior under multi-axial compression (Kittinun *et al.* 2010), and interface performance (Wu and Han 2010). Some new types of structures employing UHPCC were developed recently mainly based on bridge structures. The first building made by UHPCC material was constructed in Masselar, France in 2010 (Patrick Mazzacane *et al.* 2013).

Design of a hybrid pier with UHPCC permanent form is proposed by Wu *et al.* (2011). In this design proposal, UHPCC tubes act as permanent formworks at the construction stages and as hybrid elements at the service stages and this is described as multifunctional permanent formwork. Structural behaviors of the UHPCC hybrid composite column under axial compression and flexure are studied in this paper with proposed simplified theoretical model. Numerical analysis is carried out to validate the accuracy of the theoretical model and formulas proposed in this paper. Uniaxial compression tests of short hybrid columns are used to verify the numerical model. Comparisons of the ultimate load between the hybrid column and normal RC column show that the loading capacity is considerably improved. The minimal wall thickness of the UHPCC tube is recommended. These studies may provide a design reference for the design and application of UHPCC hybrid structures.

2. Mechanics model

2.1 Constitutive model of UHPCC

According to the results of the uniaxial tensile tests and cylinder splitting tests, the tensile strength of UHPCC with compressive strength 120 MPa is about 6 to 15 MPa, which is dependent on fiber parameters such as the steel fibers volume fraction. This tensile strength is about 3 to 8 times that of normal concrete. Deformation of UHPCC under uniaxial tension can be divided into four stages, i.e., the initial quasi linear elastic stage, the strain hardening stage, the softening stage, and the fiber pulling-out and crack localization stage. For simplification and conservative analysis, the low boundary 6 MPa is used as the tensile strength of the UHPCC in the analysis. The strain hardening region is simplified as an ideal plastic model here.

The compressive strength is limited to 120 MPa for UHPCC permanent form designs. The compressive design strength is considered to be 100 MPa with a uniform modulus 45 GPa and Poison ratio 0.18. The Young’s modulus of elasticity of UHPCC can be expressed as (ACI

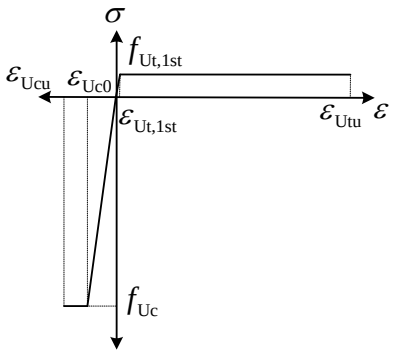

Fig. 1 Simplified tensile and compressive stress-strain model of UHPCC

Table 1 Parameters of the UHPCC tensile constitutive model

Parameter	$f_{Ut,1st}$	$\varepsilon_{Ut,1st}$	ε_{Uc0}	f_{Uc}	ε_{Ucu}
Value	6	0.0001	0.002-0.004	135	0.0043

Table 2 Mix compositions of UHPCC (kg/m3)

Cement	Silica fume	Filling powder	Fine sand	Super Plast.	Water	Expan. agent	Defoamer	Steel fiber
789.75	197.44	157.95	868.72	31.59	197.44	3.95	3.95	102.41

Committee 363 1992, Ma *et al.* 2004, Benjamin 2005, 2007)

$$E_U = 3840\sqrt{f_{Uc}'} \tag{1}$$

Where, f_{Uc}' is the compressive strength of a UHPCC cylinder specimen with diameter 100mm and height 200 mm. E_U is the Young's modulus of elasticity of UHPCC. This simplification shown in Fig. 1 agrees with the model of UHPCC proposed by FHWA Report (Benjamin 2006). The model parameters of a corresponding axial tension test are shown in Table 1.

2.2 Mixing of UHPCC with compressive strength 120Mpa

Mixing compositions of UHPCC with compressive strength 120 MPa are shown in Table 2. Fine silica sand is substituted with normal sand from the Songhua River to reduce the material cost. The volume fraction of steel fiber is 2%. Precise information on the composite materials and mixing technique of UHPCC can be obtained from (Wu and Zhao 2012).

2.3 Normal concrete and reinforcing steel

Normal Concrete (NC) with compressive strength 30 MPa and Reinforcing Steel (RS) of HRB335 with tensile strength 300 MPa are considered in the UHPCC hybrid column. The axial stress-strain relations of concrete and reinforcing steel are shown in Figs. 2-3. The idealized uniaxial tensile stress-strain relationships is used for reinforcing steel. The two stages' uniaxial compressive stress-strain relationships of NC can be written as

$$\sigma_c = \begin{cases} f_c\left[1-\left(1-\dfrac{\varepsilon}{\varepsilon_0}\right)^n\right] & 0 < \varepsilon \le \varepsilon_0 \\ f_c & \varepsilon_0 < \varepsilon \le \varepsilon_c \end{cases} \tag{2}$$

Where, f_c is the ultimate compression strength of normal concrete. ε_0 is the peak strain and ε_{cu} is the ultimate compression strain.

3. Structural behaviors of the hybrid column under compression and flexure

The coupled loads acting on the hybrid column are modeled as a fixed compression force with an eccentricity, in which the flexural moment is modeled as an eccentric load. According to the stress state of the cross section, large eccentricity and small eccentricity can be classified. First, the critical state between the two states is illustrated here.

3.1 Critical state analysis

Initially, the cross section of a UHPCC hybrid pier is in a quasi-linear elastic state and the micro crack can be omitted until the strain in the UHPCC tension zone is equal to the first cracking strain. The occurrence of the core concrete cracking depends on its cross sectional geometric character. With increasing loads, the main crack propagates continuously, accompanied by multiple cracks. Strain on the reinforcing bar in the compression zone is also increased. When the reinforcing bar in the compression zone yields, core concrete in compression will reach its ultimate state and the reinforcing bar in the tensile zone will also yield. This state is the critical state between large and small eccentric compression of UHPCC hybrid columns, as shown in Fig. 2.

3.2 Failure stage analysis of the hybrid column with large eccentricity

The failure process of UHPCC hybrid piers with large eccentric loads can be divided into four stages, i.e., the initial elastic stage, the strengthening stage, the yield stress stage, and the strengthening stage of the UHPCC compression zone.

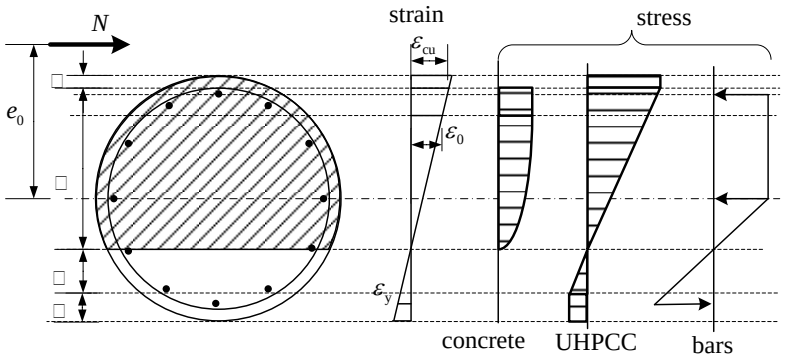

Fig. 2 Critical state of eccentric compression

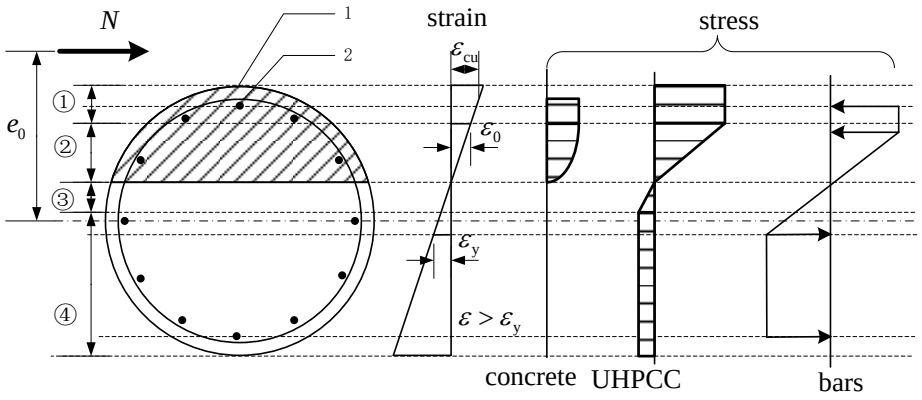

Fig. 3 Diagram of large eccentric compression hybrid column

The initial elastic stage ends at the appearance of a crack in the UHPCC tensile zone. The initial crack may develop into the final major crack. In the strengthening stage, the main crack develops continuously accompanied by multiple cracking. The tensile stress of the steel bars increases until the initial yield state. The yield stress stage starts with the bars tension yielding and ends at the compressive yield strength of the concrete. The compressive bars yield simultaneously. In the strengthening stage, for part 1 and 2 to simultaneously reach their maximum stain depends on the cross section size and the thickness of the UHPCC tube (see Fig. 3). Axial cracks in the UHPCC indicate the end of this stage and the structure is broken. The stress and strain on the cross section are shown in Fig. 3.

Finally, Part 2 of the UHPCC reaches the ultimate compression stress. The ultimate compression strain of the UHPCC is almost the same as the NC core because slippage at the interface is negligible. In this paper, it is assumed that the concrete is not broken when Part 2 reaches the ultimate compression strain, and the UHPCC in Part 1 is in the ultimate compression strain for calculating simplification.

3.3 Failure process analysis of the hybrid column with small eccentricity

The failure process of UHPCC hybrid piers with small eccentric loads can also be divided into three stages, i.e., the elastic stage, the yield stage, and strengthening stage with cracking. If the bars are centro-symmetric, the cross section may be in tension on one side and in compression on the other side, or the whole section may be in compression.

The elastic stage ends when the strain on Part 1 in Fig. 4 reaches the ultimate compression state. Part 2 can be tensile or compressive, and the UHPCC does not reach the first cracking strain and the compressive steel bars do not yield. The yield stage begins with the strain of Part 1 reaching compression yield strain and ends with the UHPCC in Part 1 or the concrete in Part 3 reaching the ultimate compression. The stress of the bars in Part 3 has reached the compression yield stress by the end of Stage 1. However, the materials at the far side do not reach the yield state. In the cracking and strengthening stage, if the UHPCC in Part 1 cracks first, the cracks develop towards Part 2 and Part 3. If the concrete in Part 3 cracks first, the cracks develop towards Part 2 and Part 1. All the cracks are longitudinal. However, the materials at the far side do not break. The distributions of the stress and strain in the cross section are shown in Fig. 4.

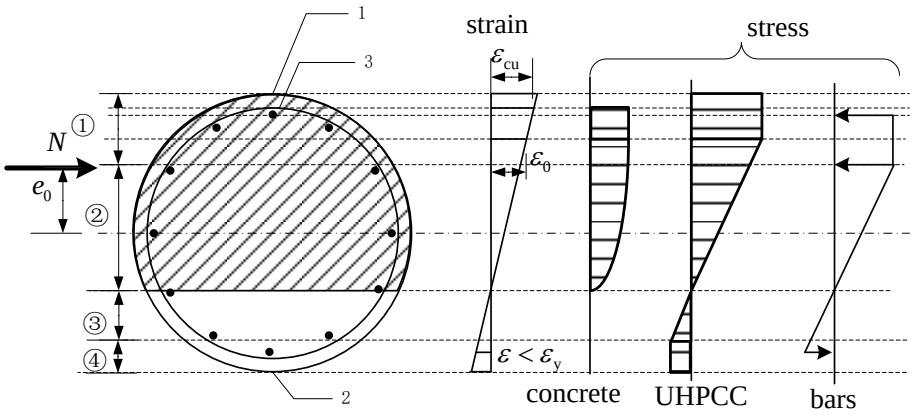

Fig. 4 Diagram of small eccentric compression hybrid column

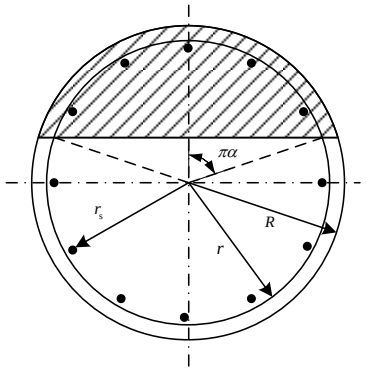

Fig. 5 Cross section of the UHPCC hybrid pier with uniform reinforcing bar

3.4 Proposed simplified unified formula for engineering designs

Analytical expression for the loading capacity of UHPCC hybrid columns based on the stress equilibrium theory will be very complex and tedious and is not appropriate for engineering calculations and designs. Based on the simplified formula in the constitution of concrete structure code (China, GB 50010-2010) (Design code 2010), a unified formula for UHPCC hybrid columns is proposed as shown in Fig. 5.

The contributions of core concrete and reinforcing bars to the structural loading capacity can be written as

$$N_{c+s} = \alpha\alpha_1 f_c A_c \left(1 - \frac{\sin 2\pi\alpha}{2\pi\alpha}\right) + (\alpha - \alpha_t) f_y A_s \tag{3}$$

Here, α is the ratio of central angle (rad) corresponding to compression zone over 2π. α_t is the ratio of longitudinal tensile reinforcing bar area over the total longitudinal reinforcing bar area. When α>0.625, α_t=0 and when $\alpha \leq 0.625$, $\alpha_t \leq 1.25\text{-}2\alpha$.

The contributions of the UHPCC to the loading capacity can be divided into two parts. The first part is from the compressive zone of the UHPCC tube. This calculation follows the rule for a

concrete member with a ring form in the code (Design code 2010). In this part, the ratio of the rectangular stress block in the UHPCC compressive zone over the axial compressive strength is induced and marked as α_{U1}. The second part is the contribution from the tensile zone of the UHPCC tube. The calculation of this part is derived from the force calculation of a reinforcing bar in the tension zone.

$$N_{\mathrm{U}} = \alpha\alpha_{\mathrm{U1}} f_{\mathrm{Uc}} A_{\mathrm{U}} + \left(\alpha - \alpha_{\mathrm{t}}\right) f_{\mathrm{Ut}} A_{\mathrm{U}} \tag{4}$$

Here, α_{U1} is the ratio of the rectangular stress block in the UHPCC compressive zone over the axial compressive strength and equals 0.94 or 0.90.

Thus, the uniform formula for the loading capacity for a UHPCC hybrid column with a circular cross section can be written as

$$\begin{aligned} N &= N_{\mathrm{c+s}} + N_{\mathrm{U}} \\ &= \alpha\alpha_{\mathrm{U1}} f_{\mathrm{Uc}} A_{\mathrm{U}} + \alpha\alpha_1 f_{\mathrm{c}} A_{\mathrm{c}} \left(1 - \frac{\sin 2\pi\alpha}{2\pi\alpha}\right) + \left(\alpha - \alpha_{\mathrm{t}}\right) f_{\mathrm{y}} A_{\mathrm{s}} + \left(\alpha - \alpha_{\mathrm{t}}\right) f_{\mathrm{Ut}} A_{\mathrm{U}} \end{aligned} \tag{5}$$

$$\begin{aligned} N\eta e_{\mathrm{i}} = {} & \alpha_{\mathrm{U1}} f_{\mathrm{Uc}} A_{\mathrm{U}} \left(R + r\right) \frac{\sin \pi\alpha}{2\pi} + \frac{2}{3} \alpha_1 f_{\mathrm{c}} A_{\mathrm{c}} r \frac{\sin^3 \pi\alpha}{\pi} \\ & + \left[f_{\mathrm{y}} A_{\mathrm{s}} r_{\mathrm{s}} + 0.5 f_{\mathrm{Ut}} A_{\mathrm{U}} \left(r + R\right) \right] \frac{\sin \pi\alpha + \sin \pi\alpha_{\mathrm{t}}}{\pi} \end{aligned} \tag{6}$$

In which, e_i is the total initial eccentricity calculated by the flexure moment and $e_i=e_0+e_a$. e_0 is the eccentricity of the axial force from the section center. e_a is the additional eccentricity and equals the maximal value of 20mm and 1/30 of the section dimension in the eccentric direction. η is the magnification factor of the eccentricity and the formula can be written as

$$\eta = 1 + \frac{1}{1400 e_{\mathrm{i}} / \left(r + r_{\mathrm{s}}\right)} \left(\frac{l_0}{2R}\right)^2 \zeta_1 \zeta_2 \tag{7}$$

With $\zeta_1=0.5(f_cA_c+f_{Uc}A_u)/N$ and $\zeta_2=1.15\text{-}0.01\ l_0/(2R)$. Here, ζ_1 is the section curvature modification factor of the eccentrically compressive member and equals 1.0 when $\zeta_1>1.0$. ζ_2 is the effect factor of the slenderness ratio on the section curvature and equals 1.0 when $l_0/R<15$. When the thickness of the UHPCC tube is equal to 0, the uniform formula regress to the formula for a reinforced concrete column with a circular cross section proposed in the code (Design code 2010).

3.5 Calculations and analysis

This analysis considers a typical UHPCC hybrid pier with an effective length of 10m, outside radius R=750 mm and inside radius r =700 mm. Sixteen HRB335 reinforcing bars with strength of 300 MPa and diameter of 20 mm were placed in the core normal concrete. The compressive strength of the core concrete is 30 MPa. The effective compressive strength of the UHPCC is 135 MPa and the bending strength is 18 MPa. The radius of the reinforcing bar ring is 0.68 m. Other parameters are given in Table 1.

Parameter η is assumed to be 1.0 at first. Then, all possible values of the moment and axial force can be solved and listed with the value of α, which can be solved. The required combined values of the moment and axial force can be found in the table. For example, the axial force

Table 3 Theoretical results of the simplified model

α	α_t	N (kN)	M (kNm)	e_i (mm)	e_0 (mm)
1/30	1.18	-2.61E+03	2.21E+02	-85	-60
1/15	1.12	-1.56E+03	9.49E+02	-608	-273
1/10	1.05	-3.83E+02	1.76E+03	-4599	-243.5
2/15	0.98	9.84E+02	2.68E+03	2723.1	1641
1/6	0.92	2.59E+03	3.71E+03	1432	943.7
1/5	0.85	4.47E+03	4.84E+03	1082	758.7
7/30	0.78	6.66E+03	6.05E+03	908.3	665
4/15	0.72	9.17E+03	7.30E+03	796.4	600.7
3/10	0.65	1.20E+04	8.55E+03	712.4	547.9
1/3	0.58	1.51E+04	9.72E+03	642.7	500.2
11/30	0.52	1.85E+04	1.08E+04	581.2	454.6
2/5	0.45	2.22E+04	1.16E+04	524.6	410
13/30	0.38	2.60E+04	1.23E+04	471.5	366
7/15	0.32	3.00E+04	1.26E+04	421	322.7
1/2	0.25	3.40E+04	1.27E+04	372.8	280.2
8/15	0.18	3.81E+04	1.24E+04	326.9	238.9
17/30	0.12	4.20E+04	1.19E+04	283.3	199.1
3/5	0.05	4.59E+04	1.11E+04	242.3	161.3
19/30	0	4.95E+04	1.01E+04	204.4	125.9
2/3	0	5.27E+04	8.95E+03	169.9	93.6
7/10	0	5.56E+04	7.70E+03	138.4	64.1
11/15	0	5.83E+04	6.42E+03	110.1	37.7
23/30	0	6.06E+04	5.16E+03	85.2	14.7
4/5	0	6.26E+04	3.99E+03	63.8	-5
5/6	0	6.43E+04	2.94E+03	45.7	-21
13/15	0	6.57E+04	2.02E+03	30.7	-33
9/10	0	6.69E+04	1.24E+03	18.5	-0.042
14/15	0	6.79E+04	5.88E+02	8.7	-0.048
29/30	0	6.88E+04	3.94E+02	0.6	-0.05
1	0	6.95E+04	-4.46E+03	-6	-0.048

corresponding to the maximal moment can be looked up and the moment corresponding to zero axial force can also be looked up. Before the eccentricity is to be solved, N and e_i must be solved first. η can be obtained by substituting N and e_i into Eq. (7).

First, α is assigned values in the interval 0 to 1, as shown in the first column of Table 3, and α_t can be obtained by α_t=1.25-2α. Each value of α corresponds to an equilibrium state of the cross section. The corresponding resistances of axial force N and moment M can be solved with Eqs. (5)-(6) and are listed in the third and fourth columns of Table 3. The combination of moment and axial force in corresponding equilibrium states can be checked in this table. For example, axial force corresponding to maximal moment can be checked and moment corresponding to zero axial force, i.e., a pure flexural state, can also be checked. Corresponding allowable eccentricity can be solved by an iterative method. Parameter η_0 is assumed to be 1.0 at first. Allowable eccentricity e_i

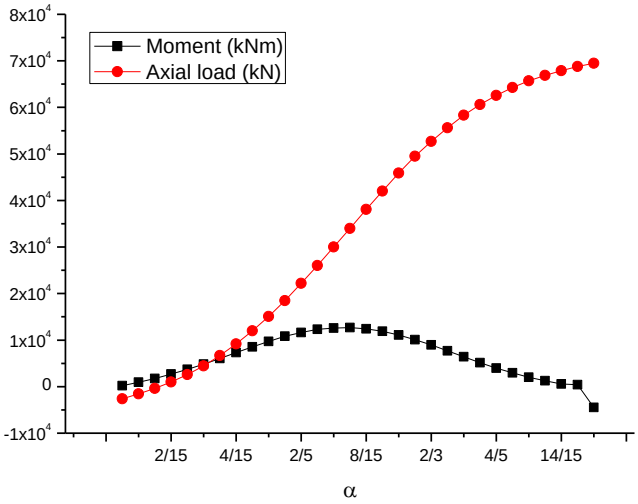

Fig. 6 Results of a UHPCC hybrid pier with thickness 50 mm under eccentric loading

can be solved by Eqs. (5)-(6). By substituting e_i into Eq. (7), the corresponding parameter η_1 can be solved. By comparing it with the previous value of η_0, η can be determined if the absolute D-value of $|\eta_1-\eta_0|\leq 0.5$. Otherwise, the iteration process cannot be completed until the D-value is satisfied. With, $e_i=e_0+e_a$, e_0 can finally be solved as shown in Table 3 and Fig. 6.

The results show that the maximal moment is 1.27E+07N·m when the angle ratio α equals 0.5 with an eccentricity of 280 mm and an axial compressive force of 3.40E+07N. The full section is in compression when the angle ratio is 1.0 with axial force equal to 6.95E+07N and these results agree well with the results for a UHPCC hybrid pier under axial compression (Wu and Zhao 2011).

Although the loading capacity of the longitudinal reinforcing bars is considered in the calculations for a UHPCC hybrid pier under eccentric compression, the contributions of the reinforcing bars on the structural loading capacity are very small. Therefore, reinforcing bars are not taken into account when calculating the structural loading capacity. Since the properties of the concrete and the UHPCC materials are not idealized, structural reinforcement is still necessary to control the stress distribution, especially for structural behaviors under in a plastic state.

3.6 Numerical simulations

Due to the difficulties resulting from large dimensions in hybrid column loading tests, a recursive method is used here to verify the numerical model used to verify the theoretical simplified formula in the case of uniaxial compression.

3.6.1 Recursive verification of the hybrid column test

Four groups of the specimens are designed and each group has three specimens. In total, twelve specimens are loaded in the tests. Each specimen is named UN(H)-t, according to its height (H) and thickness (t). The geometric dimensions of the hybrid specimen are listed in Table 4, in which OR, IR, H and t represent the outside radius, inside radius, height, and thickness of the UHPCC tube, respectively. The test results of the cracking capacity and ultimate loading capacity are also listed in Table 4. Loading processes of the specimen are shown in Fig. 7.

Table 4 Test specimen of the short hybrid column

Specimen	OR (mm)	IR (mm)	H (mm)	*t* (mm)	Cracking load (kN)	Ultimate load (kN)
UN(400)-15	96	81	400	15	900	1707
UN(400)-32	96	64	400	32	1200	2635
UN(400)-42	96	54	400	42	1500	3200
UN(300)-23	77	54	300	23	990	1401

(a) UN(400)-15 (b) UN(400)-32 (c) UN(400)-42 (d) UN(300)-23

Fig. 7 Loading test of the UHPCC-NC hybrid column

Table 5 Material parameters

Material	Poison ratio	*E* (GPa)	Ultimate comp. strain	Comp. strength (MPa)	Cracking strain	Cracking stress (MPa)	Ultimate tensile strain	Rupture strength (MPa)
UHPCC	0.18	50	0.0043	135	0.00016	8.1	0.01	18
NC	0.2	30	0.0036	30	0.00012	1.8	0.00014	2.2
Steel bar	0.3	200	0.01	335	——	335	0.01	——

A smeared cracking model was used here. The material parameters are listed in Table 5. A step-by-step loading method was used. Element C3D8R was selected for the simulation. Pin-fixed boundary conditions were selected for the interface between the UHPCC and NC sections. The first cracking load can be obtained.

Numerical and test results of the specimens are shown in Fig. 8 and the comparisons indicate that the numerical results agree well with the test results.

3.6.2 Numerical results of large dimension UHPC hybrid pier

A typical UHPCC hybrid pier under compression and flexure loading described in Section 3.5 is simulated here. Material parameters for the simulation are listed in Table 5. The eccentricity is calculated and equals 284 mm. The load range is from 0 to 7.04E+07N. The numerical model parameters are described in 3.6.1. Stress, strain and, deformation nephograms are shown in Figs. 9-12.

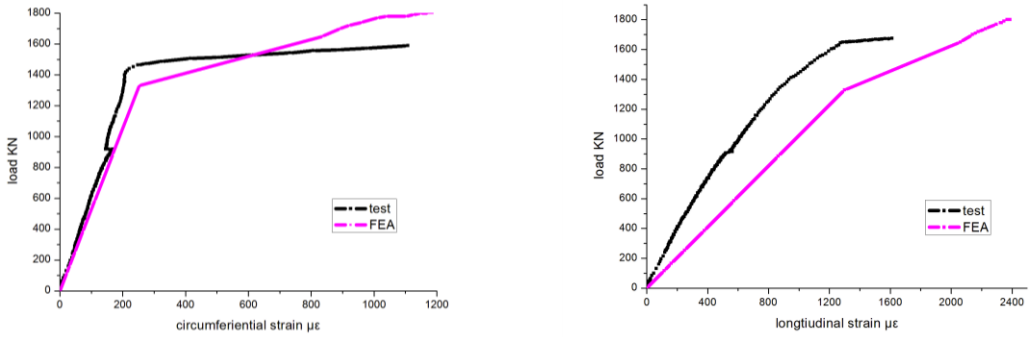

(a) Results of specimen UN(400)-15

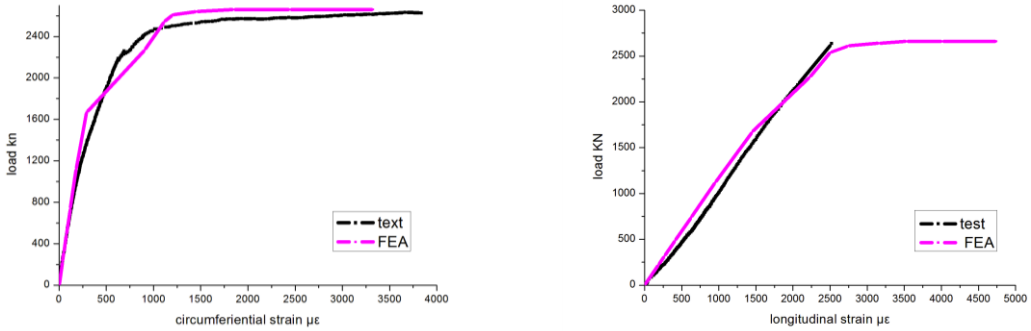

(b) Results of specimen UN(400)-32

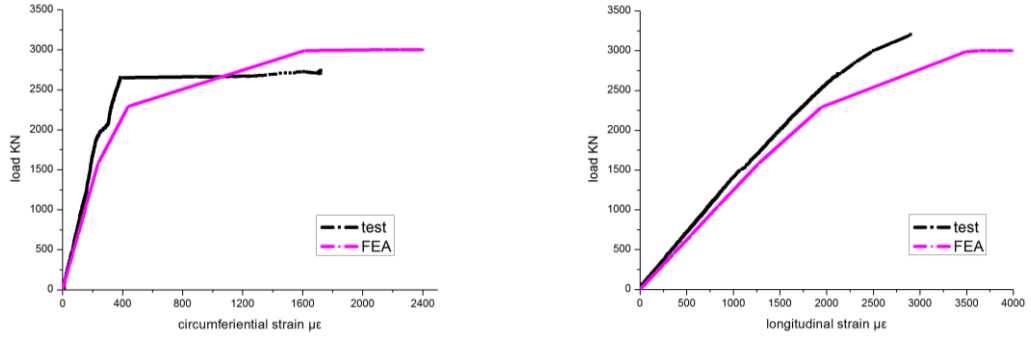

(c) Results of specimen UN(400)-42

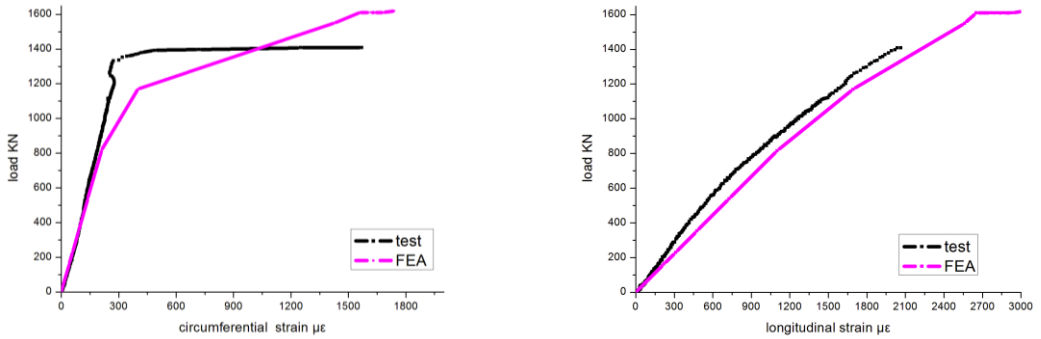

(d) Results of specimen UN(300)-23

Fig. 8 Comparisons of the numerical model and test results

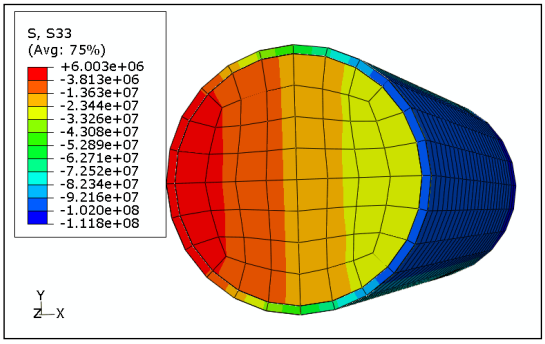

Fig. 9Axial stress in central section

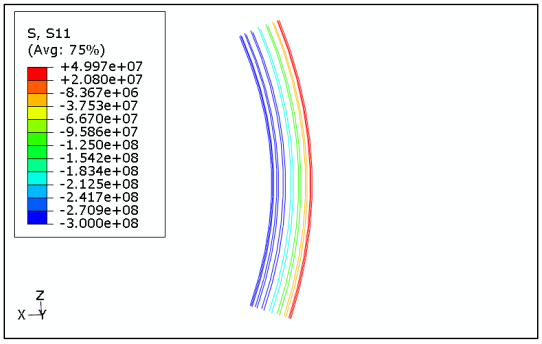

Fig. 10 Stress of reinforcing bars

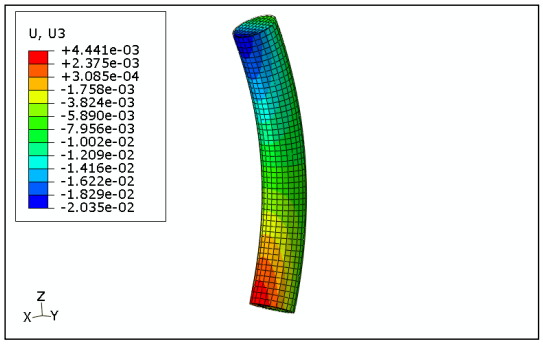

Fig. 11 Axial displacement

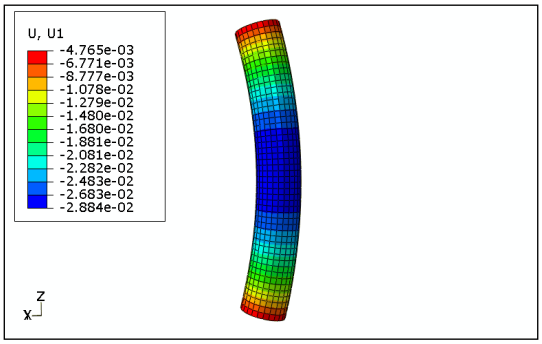

Fig. 12 Flexural deflection

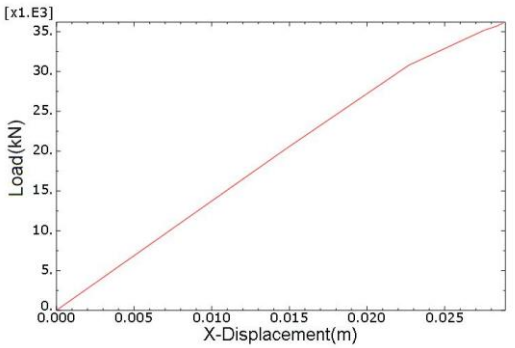

Fig. 13 Deflection-load in the direction of eccentricity

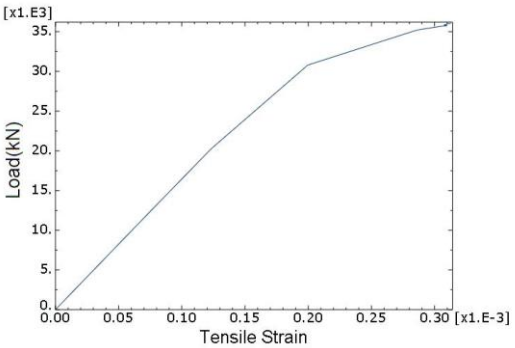

Fig. 14 Strain-load of UHPCC tensile zone

Fig. 13 shows that the first knee point corresponds to the first cracking state of the UHPCC and the second knee point corresponds to the compressive plastic state. Cracking in the UHPCC tensile zone does not affect the structural lateral deflection.

Fig. 14 shows that the UHPCC tensile zone enters a subsequent plastic stage after the first tensile cracking. Fig. 15 shows the final ultimate state, which is the main reason for eccentric structural failure. At this stage, reinforcing bars show flow rate characteristics. Although the compressive strain of the UHPCC does not reach the ultimate limit strain, to realize convergence is very difficult and the structure is considered to fail.

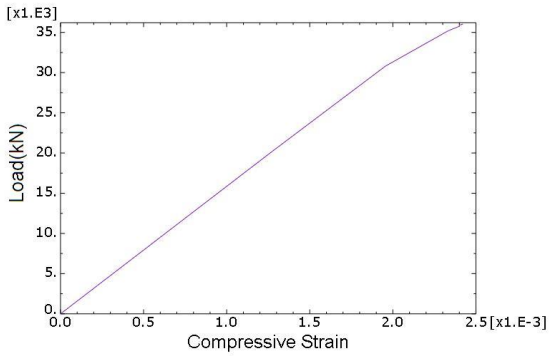

Fig. 15 Strain-load of UHPCC compressive zone

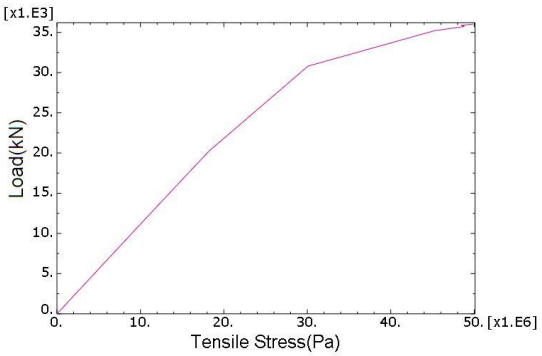

Fig. 16 Stress-load of tensile reinforcing bars

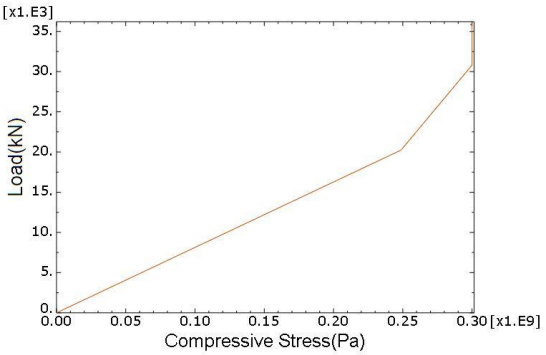

Fig. 17 Stress-load of reinforcing bar in compressive zone

Figs. 16-17 show the relationships between the loads and stresses of the reinforcing bars. The first knee point corresponds to the tensile crack of the UHPCC. The second knee point of the reinforcing bars curve corresponds to the compressive plastic state of UHPCC. The compressive reinforcing bar yields simultaneously with the onset of UHPCC plastic deformation. This failure type is the same as the large eccentric compression failure.

The results show that the structure reaches large plastic deformation when the load is 3.60E+07N, as shown in Figs. 15-19. This load value is considered the failure load during numerical simulations and is also close to the theoretical result of 3.40E+07N. Therefore, the loading capacity of a UHPCC hybrid pier can be predicted using this method. Numerical simulations results were slightly greater than the theoretical results due to the tensile stress effect of the concrete being included in the numerical simulations but omitted in the theoretical model.

The deviations of the compressive and tensile regions in the cross section between theoretical and numerical results are rather large. The theoretical central angle ratio of the compression-tension region is 0.5, which is different from the numerical results shown in the stress and strain nephograms. This is a result of stress block simplification in the simulation. In the simplified method, the tensile region is assumed to be at the ultimate limit and the compressive region is at the equivalent yield. This simplification is different from the numerical analysis process.

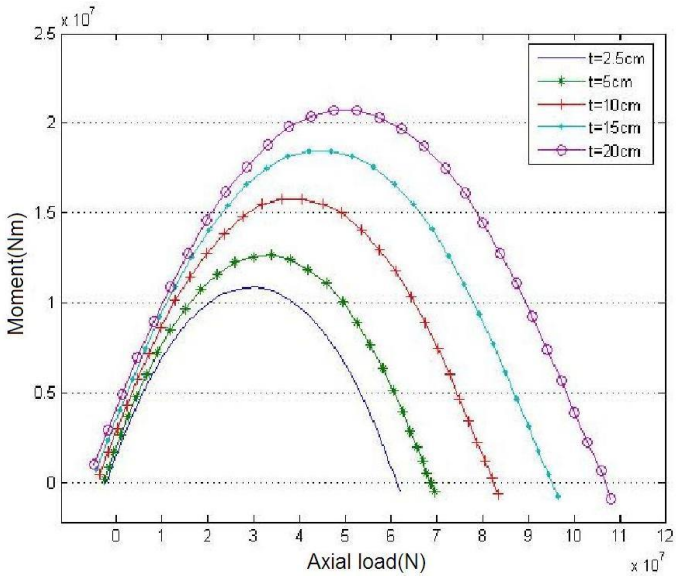

Fig. 18 N-M envelope diagrams

Table 6 Comparisons of moment and axial force with different thickness

thickness *t* (mm)	angle	Theoretical flexural capacity (kNm)	Theoretical axial loading capacity (kN)	Eccentric distance (m)	Numerical axial loading capacity (kN)	Deviation percentage	Improvement percentage
(1)	(2)	(3)	(4)	(5)	(6)	(7)	(8)
0	1/2	9.03E+06	2.69E+04	0.243	2.244E+04	19.687%	
25	1/2	1.09E+07	3.05E+04	0.265	3.185E+04	4.215%	41.93%
50	1/2	1.27E+07	3.44E+04	0.280	3.603E+04	4.629%	60.57%
100	1/2	1.58E+07	3.81E+04	0.298	4.509E+04	15.400%	100.95%
150	7/15	1.849E+07	4.18E+04	0.346	4.495E+04	7.018%	100.31%
200	7/15	2.07E+07	4.52E+04	0.346	5.470E+04	17.367%	143.78%

3.7 Effect of the UHPCC tube thickness

Theoretical results with different thickness are calculated as shown in Fig. 18. The results indicate that the axial loading capacity and flexural capacity increase linearly with the UHPCC tube thickness. These curves are also envelope diagrams of the moment and axial force for UHPCC hybrid columns with different tube thicknesses. The area inside the curve is the safety region and outside is the failure region.

Numerical results with different tube thickness are shown in Table 6, which is recommended as a preliminary reference for UHPCC hybrid column designs. Typical tube thicknesses of 0 mm, 25 mm, 50 mm, 100 mm, 150 mm and 200 mm are considered and the hybrid column with thickness 0mm corresponds to a traditional normal concrete column. Loading positions are specified as the eccentricity corresponding to the maximum moment.

It can be seen from the comparisons that the theoretical results agree well with the numerical simulations as shown in Fig. 19, especially for a thin UHPCC tube. When the design thickness of

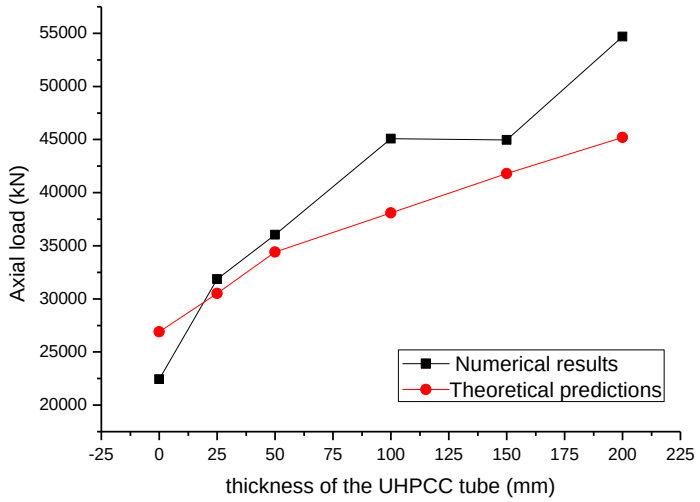

Fig. 19 Comparisons of axial loading capacity

the UHPCC tube is 25 mm, the difference between the theoretical and numerical results is only 4.215%. However, the difference increases with the thickness of the UHPCC tube. When the design thickness is 150mm, the difference is 7.018%, which is caused by the rapid changing of the eccentricity from tube thickness 100 mm to 150 mm. The corresponding moment is enlarged and the estimated maximal axial force is low. When the design thickness is 200 mm, the difference is 17.367%. The difference is a result of neglecting the confinement of the UHPCC tube in the theoretical model and formula. As a result, the theoretical results are slightly smaller.

Since the UHPCC confinement effects are not considered in the proposed theoretical model, the theoretical formula can also be used to predict a normal concrete member. When the UHPCC tube thickness is reduced to zero, the hybrid column is transformed into a normal concrete structure without any confinement. Corresponding numerical simulations are smaller than the theoretical results, in which stirrups are included in the normal concrete column. Although confinement effects in a UHPCC tube are not included in the theoretical formula, the proposed formula is still applicable here for hybrid columns with thicknesses of less than 50mm. In addition, calculations based on the simplified theoretical model agree well with the results based on the code (Design code 2010). Therefore, the formula proposed in this paper is universal and applicable, not only for hybrid columns, but also for traditional RC columns under eccentric compression.

The improvements to structural loading capacity provided by UHPCC tubes are shown in column (8) of Table 6, with different tube thicknesses. The minimal thickness of the UHPCC tube is limited to 20mm. It can be shown from the comparisons that the structural loading capacity under eccentric compression is improved by about 40% due to the hybrid effects.

4. Conclusions

The simplified formula proposed is a unified formula for UHPCC hybrid column and normal reinforced concrete column, and it is conservative and suitable for engineering designs when the thickness-radius ratio is equal to or less than 1:15.

The improvements to loading capacity from the UHPCC tube hybrid effects are significant compared with traditional normal RC columns. The minimum thickness of the UHPCC tube is 20mm.

Each combinations of axial force and moment with allowable eccentricity are listed in the Table 3. The loading capacity can be checked conveniently using this table and complicated calculations can be avoided.

Acknowledgements

The authors would like to thank the National Natural Science Foundation of China (51008088), the Fundamental Research Funds for the Central Universities (Grant No. HIT. NSRIF. 2013112), Harbin City Science and Technology Innovation Talents Special Funds (2011RFLXG014), and Heilongjiang Province Natural Science Fund (E200911) for providing funding to this project, the National Key Technology Research and Development Program of China under Grant No. 2011BAJ10B0102, and the Scientific Technical Plan of The Ministry of Housing and Urban-Rural Development of China (2010-K2-23) for the supporting the authors' work described herein.

Notations

f_{Uc}' : cylinder compressive strength of UHPCC.
E_U: Young's modulus of elasticity of UHPCC.
f_c: ultimate compression strength of normal concrete.
ε_0: peak compressive strain of normal concrete.
ε_{cu}: ultimate compression strain.
α: ratio of central angle corresponding to compression zone over 2π.
α_t: ratio of longitudinal tensile reinforcing bar area over the total longitudinal bar area
α_{U1}: ratio of the rectangular stress block in the UHPCC compressive zone over the axial compressive strength.
e_i: total initial eccentricity calculated by the flexure moment.
e_0: eccentricity of the axial force from the section center.
e_a: additional eccentricity.
η: the magnification factor of the eccentricity.
ζ_1: section curvature modification factor of the eccentrically compressive member.
ζ_2: effect factor of the slenderness ratio on the section curvature.

References

Behloul, M. (2007), "HPFRCC field of applications: Ductal recent experience", *5th High Performance Fiber Reinforced Cement Composite (HPFRCC5)*, Mainz, Germany, July.

Benjamin, A.G. (2005), "Characterization of the behavior of ultra-high performance concrete", Ph.D. Dissertation, University of Maryland, MD.

Benjamin, A.G. (2007), "Compressive behavior of ultra-high performance fiber-reinforced concrete", *ACI Mater. J.*, **104**(2), 146-152.

Cavill, B. and Chirgwin, G. (2003), "The world's first ductal road bridge sherpherds gully creek bridge, NSW", *21st Biennial Conference of the Concrete Institute of Australia*, Brisbane, Australia, July.
Design code (2009), *Constructurn Manual For Reactive Powder Concrete Member*, China Railway Publishing House, Beijing. (In Chinese)
Design code (2010), *Code for design of concrete structures (GB 50010-2010)*, China Architecture & Building Press, Beijing. (In Chinese)
Graybeal, B.A. (2006), "Structural behavior of ultra-high performance concrete prestressed I-girders", FHWA-HRT-06-115. August.
Graybeal, B., Hartamann, J. and Perry, V. (2004), "Ultra-high performance concrete for highway bridge", *FIB Symposium*, Avignon, April.
Kittinun, S., Sherif, E.T. and Gustavo, P.M. (2010), "Behavior of high performance fiber reinforced cement composite under multi-axial compressive loading", *Cement Concrete Compos.*, **32**, 62-72.
Ma, J., Dehn, F., Tue, N.V., Orgass, M. and Schmidt, D. (2004), "Comprarative investigations on ultra-high performance concrete with and without coarse aggregates", *Proceedings of the International Symposium on Ultra-High Performance Concrete*, Kassel, Germany, September.
Maalej, M. and Li, V.C. (1995), "Introduction of strain hardening engineered cementitious composites in design of reinforced concrete flexural members for improved durability", *ACI Struct. J.*, **92**(2), 167-176.
Mazzacane, P, Ricciotti, R., Teply, F., Tollini, E. and Corvez, D. (2013), "MUCEM: The builder's perspective", *Proceedings of the RILEM-FIB-AFGC Int. Symposium on Ultra-High Performance Fiber-Reinforced Concrete*, Marseille, France, October.
Okuma, H. *et al.*. (2006), "The first highway bridge applying ultra high strength fiber reinforced concrete in Japan", *7th International Conference on short and medium span bridge*, Montreal, Canada, August.
Ramadoss, P. and Nagamani, K. (2008), "A new strength model for the high-performance fiber reinforced concrete", *Comput. Concrete*, **5**(1), 21-36.
Ramadoss, P. and Nagamani, K. (2013), "Stress-strain behavior and toughness of high performance steel fiber reinforced concrete in compression", *Comput. Concrete*, **11**(2),149-167.
Research report (1992), "Report on high-strength concrete (ACI 363R-92)", American Concrete Institute, Farmington Hills, Mich, 55.
Williams, E.M., Graham, S.S., Akers, S.A., Reed, P.A. and Rushing, T.S. (2010), "Constitutive property behavior of an ultra-high-performance concrete with and without steel fibers", *Comput. Concrete*, **7**(2), 191-202.
Wu, X.G. and Han, S.M. (2010), "Interface shear connection analysis of ultra-high performance fiber reinforced concrete composite girders", *J. Bridge Eng.*, ASCE, **15**(5), 493-502.
Wu, X.G., Han, S.M. and Xu, S.L. (2008), "Pseudo-strain hardening model of ultra high performance cementitious composites under flexural loading", *Acta Materiae Compositae Sinica*, **25**(2), 129-134.
Wu, X.G., Xu, S.L. and Wu, M.X. (2009), "Fracture parameters study and application of ultra-high performance fiber reinforcement concrete", *Eng. Mech.*, **26**(3), 93-98.
Wu, X.G., Jiang, X.D. and Zhao, X.Y. *et al.*. (2011), "Multiple functional permanent form for bridge gravity pier", China Patent, Publication Number: CN 201952733 U.
Wu, X.G., Zhao, X.Y. and Han, S.M. (2012), "Structural analysis of circular UHPCC form for hybrid pier under construction loads", *Steel Compos. Struct.*, **12**(2), 167-181.

CC